Electromagnetic Modeling Of The AGS A10 Injection Kicker Magnet

Roberto B. Armenta, Michael J. Barnes, *Member, IEEE*, Ewart W. Blackmore, *Member, IEEE*, Ori Hadary, Derek T. Norn, Gary D. Wait

***Abstract*— The present Alternating Gradient Synchrotron (AGS) injection kicker magnets at the A5 location were designed for 1.5 GeV proton injection. Recent high intensity runs have pushed the transfer kinetic energy to 1.94 GeV, but with an imperfect matching in transverse phase space. Space charge forces result in both fast and slow beam size growth and beam loss. A proposed increase in the AGS injection energy to 2 GeV with adequate kick strength would greatly reduce the beam losses making it possible to increase the intensity from 70 TP (70 * 10^{12} protons/s) to 100 TP. R&D studies are being undertaken by TRIUMF, in collaboration with Brookhaven National Laboratory (BNL), to design two new kicker magnets for the AGS A10 location to provide an additional kick of 1.5 mrad to 2 GeV protons. The kick strength rise and fall time specifications are 100 ns, 3% to 97%; the design goal is to achieve a field uniformity, for protons, of ±3% over 90% of the cross-sectional area of the aperture. TRIUMF has proposed a design for a 12.5 Ω transmission line kicker magnet powered by a matched 12.5 Ω pulse forming line. This paper presents the results of detailed 2D and 3D electromagnetic modeling of the kicker magnet, and a novel mathematical model of the kicker.**

***Index Terms*— kicker magnet, pulse-forming line, pulsed magnet.**

I. Introduction

THE proposed design for the Alternating Gradient Synchrotron (AGS) A10, 11 cell, transmission line kicker magnets, is based on a TRIUMF prototype 10-cell kicker [1], [2] (Fig. 1), which was based on designs originated at CERN [3], [4]. The transmission line type kicker consists of ferrite C-core sections sandwiched between high voltage (HV) capacitance plates. One C-core, together with its ground and HV capacitance plates, is termed a cell. Each cell conceptually begins and ends in the middle of the HV capacitance plates. Striplines (Fig. 1), at the input and output of the kicker, have an impedance as close as possible to that of the kicker.

Manuscript received September 19, 2005. Work supported by a contribution from the National Research Council of Canada.

R. B. Armenta is with University of Victoria, Victoria, BC, V8W 2Y2, Canada (e-mail: rarmenta@alumni.uvic.ca).

M. J. Barnes is with TRIUMF, Vancouver, BC, V6T 2A3, Canada (phone: 604-222-7308; fax: 604-222-7309; e-mail: barnes@triumf.ca).

E. W. Blackmore is with TRIUMF, Vancouver, BC, V6T 2A3, Canada (phone: 604-222-7461; fax: 604-222-7309; e-mail: ewb@triumf.ca).

O. Hadary is with University of Victoria, Victoria, BC, V8W 2Y2, Canada (e-mail: ohadary@alumni.uvic.ca).

D.T. Norrn is with University of Victoria, Victoria, BC, V8W 2Y2, Canada (e-mail: derekn@uvic.ca).

G.D. Wait is with TRIUMF, Vancouver, BC, V6T 2A3, Canada (phone: 604-222-3211; fax: 604-222-7309; e-mail: wait@triumf.ca).

TABLE I
EXISTING A5 AND PROPOSED A10 KICKER PARAMETERS FOR 2 GEV PROTONS

Parameter	Existing A5	Proposed A10
Deflection angle	2.48 mrad	1.5 mrad
Gap height	57.15 mm	81 mm
Gap width	127 mm	137 mm
Rise time 3% to 97%	140 ns	100 ns
Fall time 97% to 3%	140 ns	100 ns
Flat-top Duration	0 to 2250 ns	0 to 1650 ns
Number of magnets	3	2
Magnetic field	24.2 mT	19.1 mT
Current	1100 A	1235 A
PFL Voltage	32.5 kV	30.9 kV
Magnet type	Lumped	Transmission line

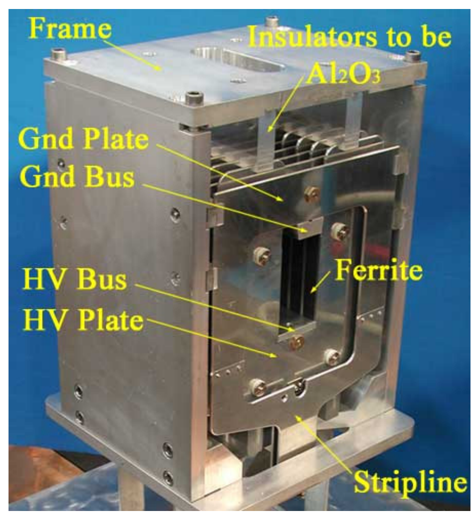

Fig. 1. Prototype TRIUMF kicker magnet.

The rise time of the field is dependent upon the rise time of the input pulse, the delay of each cell ($\sqrt{L \bullet C}$, where L and C are the inductance and capacitance per cell of the kicker magnet, respectively) and the number of cells in a kicker. To achieve rise and fall times of 100 ns (Table I) two 11 cell kickers are used, each driven by its own pulse generator, rather than one 22 cell kicker. The characteristic impedance (Z) is given by (1).

$$Z = \sqrt{L / C} \, . \qquad (1)$$

Impedance mismatches result in reflections which cause field ripple and potentially reduce the life of the thyratron switches.

A carefully matched high bandwidth system is needed to obtain the stringent pulse response requirements. Hence each of the two A10 systems is composed of a Pulse Forming Line (PFL) and an 11 cell traveling wave kicker magnet, connected by a matched transmission line and terminated by a matched resistor. To obtain a compact and cost efficient design a low system impedance of 12.5 Ω is chosen. Fig. 2 gives a circuit schematic for one of the kicker systems.

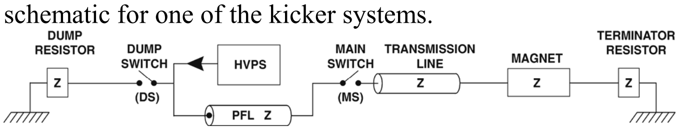

Fig. 2. Schematic circuit of one kicker magnet system.

II. 2D ELECTROMAGNETIC SIMULATIONS

The specifications for the AGS A10 kicker magnet require an aperture width (the distance between the adjacent surfaces of the HV bus and the GND bus) of 127 mm, and an aperture height (the distance between the inner surfaces of the legs of the C-core ferrite) of 81 mm (Fig. 3). The total series inductance of a central cell is determined by the aperture dimensions and can reasonably accurately be calculated from the equation: $L = \mu_0 \times w \times l / h$, (59.27 nH) where, w is the width of the aperture (127 mm for the nominal aperture), l is the length of a cell (30.06 mm), and h is the height of the aperture (81 mm).

The beam's trajectory is nominally along the z-axis. The required 1.5 mrad of horizontal beam deflection (θ_x) is provided by the magnetic $(\theta_{B,x})$ and electric $(\theta_{E,x})$ fields, and is the algebraic sum of (2) and (3).

$$\theta_{B,x} = \frac{0.3}{P} \cdot \int B_y \bullet dz \,. \tag{2}$$

$$\theta_{E,x} = \frac{c}{P \cdot \beta \cdot c \cdot 10^9} \cdot \int E_x \bullet dz \,. \tag{3}$$

where B_y and E_x are obtained from electromagnetic simulations, at given X and Y coordinates. B_y is the vertical component of the magnetic flux density in units of Tesla, dz is the arc length differential vector in units of meters, P is the beam momentum in units of GeV/c, E_x is the electric field vector in units of V/m, $\beta \cdot c$ is particle velocity and c is the velocity of light.

Electromagnetic simulations have been carried out, using 2D finite element software [5], to predict the magnetic and electric fields in the aperture of the kicker [4]. The magnetic and electric components of deflection can be arranged to either add or subtract [6], [7]. For the nominal geometry the optimum is for the electric field deflection to subtract from the magnetic field deflection [6]: in this case 81% of the aperture's cross-sectional area (CSA) has a deflection uniformity of ±3% for protons.

Further 2D simulations have been carried out to optimize deflection uniformity [4], [7] while not significantly increasing cell inductance: Fig. 3 shows the optimized geometry. The changes made are:

- Increasing the aperture width from 127 mm to 137 mm;
- Shaping of the aperture side surface of the GND bus;
- Shaping of the legs, at the GND end, of the ferrite.

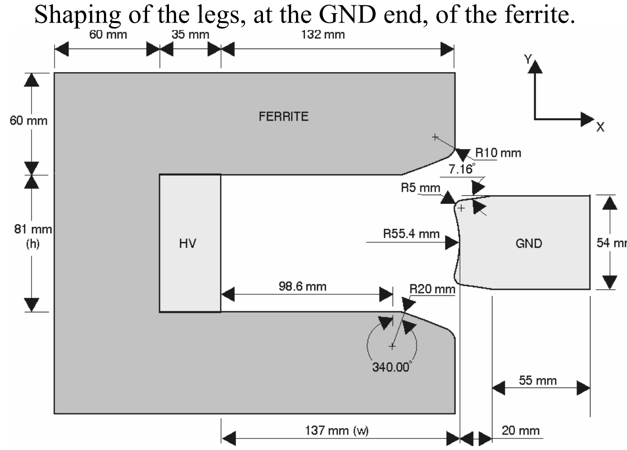

Fig. 3. Cross section of optimized aperture.

The magnetic and electric components of deflection are added, for the optimized geometry, to give the most uniform deflection [7]. Fig. 4 shows a contour plot of the resultant total deflection for protons, normalized to the deflection at the centre of the specified aperture. The deflection uniformity is within ±1%, ±2% and ±3% over 83.6%, 88.6% and 91% of the aperture CSA, respectively. From (3) since $\beta \cdot c$ is smaller for Au^{77+} than for protons, the electric field deflection is larger for Au^{77+}: for Au^{77+} the uniformity is ±1%, ±2%, ±3% over 27.2%, 74.7% and 83.4%, respectively, of the aperture CSA.

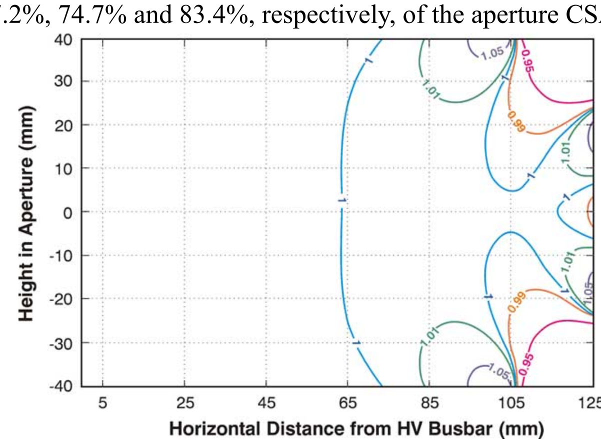

Fig. 4. Normalized contour plot of $\theta_x = \theta_{B,x} + \theta_{E,x}$, for protons, from 2D simulations, for the optimized geometry.

The predicted inductance of the optimized geometry is 62.4 nH per 30.06 mm long cell, an increase in inductance of 4.2% relative to the nominal geometry.

The above 2D simulations modeled ferrite with a constant relative permeability of 2000. The optimized geometry has also been simulated with both a realistic BH curve for the CMD5005 ferrite as well as holes for mounting the ferrite. The predicted inductance increases slightly to 62.64 nH/cell. The predicted deflection uniformity for protons is very similar to the linear 2D model and is within ±1%, ±2% and ±3% over 83.6%, 88.7% and 91.1% of the aperture CSA, respectively.

III. 3D ELECTROMAGNETIC SIMULATIONS

A. *Cell Inductance and Flux Density*

Fringe fields result in an appreciable increase in inductance per cell towards the ends of the kicker [2]. Hence in order to obtain realistic predictions it is necessary to employ a 3D code. In addition, because the excitation pulse contains high frequency components, it is important to model eddy currents. The optimized geometry has been simulated using Elektra [5], a 3D finite element code that simulates eddy currents.

Accurately simulating a magnet in 3D using a finite element code can require a large amount of memory and CPU time. In addition, the accurate simulation of eddy currents requires that there are an adequate number of finite elements per skin depth (e.g. 3), near to the surface of the conducting regions. However, due to symmetry of the kicker magnet, it is only necessary to model a quarter of the magnet (Fig. 5).

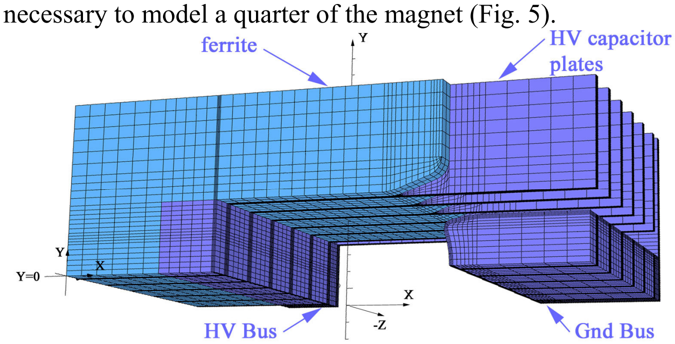

Fig. 5. Quarter model of AGS A10 kicker.

The two AGS A10 kickers will be separated by 20 mm between the outer faces of adjacent striplines. The 3D simulations, for predicting the magnetic and electric fields, have been run twice each. The first simulation is with the boundary at the stripline end of the magnet modeled at a distance of 10 mm from the stripline, to simulate the adjacent ends of the two kickers, and the second simulation is with the boundary at a distance of 157.5 mm from the stripline to simulate the opposite ends of the two kickers.

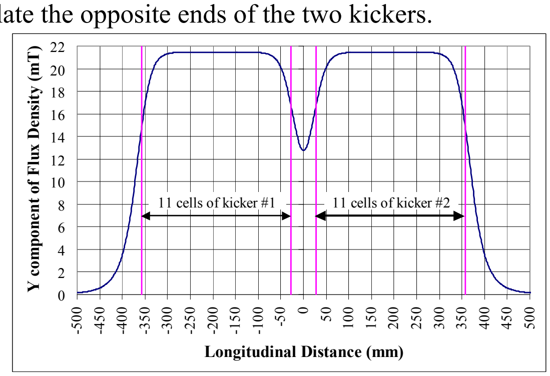

Fig. 6. Predicted Y component of flux density along centerline of specified aperture of two kickers separated by 20 mm.

Fig. 6 shows a plot of the predicted Y component of flux density along the centerline of the specified aperture. The Y component of flux density through the inner 9 cells of a kicker, at the centre of the specified width of the aperture, is within 95% of the field at the centre of a kicker: at the outer ends of the kickers (±357.5 mm) the flux density is 69% of the value at the centre of a kicker. The flux density is 10% of the central value at a distance of approximately 55 mm from the outer ends of the ferrite. At the centre between the two kickers (0 mm in Fig. 6) the flux density at the centre of the specified aperture is 60% of that at the centre of a kicker.

The self-inductance of each cell is derived from the Elektra predictions by integrating the Y component of the predicted flux density through the back yoke of the appropriate ferrite, along the Y=0 plane, and dividing the resultant flux by the total driving current. Fig. 7 shows a plot of the cell inductance versus the cell number. Cell 6 is at the centre of a kicker, cell 11 is the end of a kicker where the second kicker is adjacent, and cell 1 is the opposite end of the kicker.

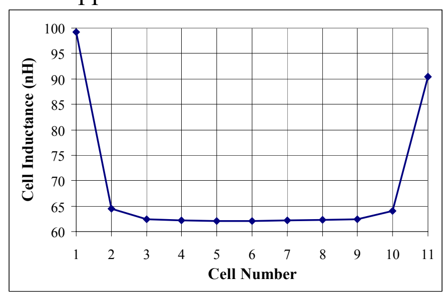

Fig. 7. Predicted cell inductance versus cell number.

The predicted inductance for the central cell, obtained from the 3D simulations, is 62.11 nH which is 0.5% less than that obtained from the, linear, 2D simulation.

The cell inductances given by the 3D simulations are:

- Cell 2 has an inductance 3.7% greater than cell 6;
- Cell 10 has an inductance 3.1% greater than cell 6;
- Cell 1 has an inductance 59.8% greater than cell 6;
- Cell 11 has an inductance 45.7% greater than cell 6.

Hence, the presence of the adjacent magnet significantly decreases the end cell inductance.

B. *Equivalent Circuit of Magnet*

Time domain analysis of the kicker system, using PSpice, is an important tool for optimizing the response of the kicker system [8]. The equivalent circuit utilized for the mathematical studies of the kicker magnet is based upon that used by the CERN PS division [3] and is shown in Fig. 8.

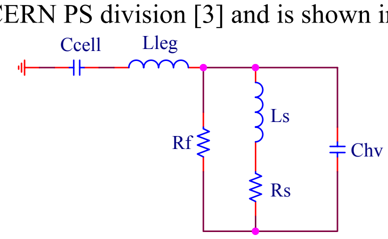

Fig. 8. Equivalent circuit of one-cell of a kicker magnet.

In Fig. 8 Ccell is the shunt capacitance to ground of each cell, Rs is the series resistance of both the HV and GND busbars associated with each cell, Chv is the parasitic capacitance between the adjacent HV capacitance plates of the kicker, and Rf simulates losses in the ferrite core of a cell. In previous mathematical models of the kicker, Ls represented the total series inductance of each cell of the kicker, as per Fig. 7, and Lleg represented both the series inductance of the legs of the HV and GND plates, between the HV and GND busbars, and negative mutual coupling between adjacent cells of the kicker magnet. The value of Lleg was difficult to quantify, however the mathematical model has been modified and Lleg can now be readily calculated. In a central cell there are no fringe fields; the presence of the adjacent cells eliminates the fringe fields and therefore reduces the total inductance of a central cell. Hence the self-inductance of a cell can be considered to be mutually coupled to the self-inductances of adjacent cells: a central cell is mutually coupled to cells on both sides, whereas an end cell is mutually coupled to a cell on only one side. For a central cell, of self-inductance L_{sf1}, the total apparent series inductance of this cell, L_{tc}, is given by:

$$L_{tc} = L_{sf1} + 2k_{12}\sqrt{L_{sf1}L_{sf2}} + 2k_{13}\sqrt{L_{sf1}L_{sf3}} . \quad (4)$$

Where L_{sf1}, L_{sf2}, and L_{sf3} are self-inductances of cells: inductances are in the order L_{sf3}, L_{sf2}, L_{sf1}, L_{sf2}, L_{sf3}. Since all cells are nominally identical $L_{sf1} = L_{sf2} = L_{sf3}$.

For the second cell in from the end of the magnet the total apparent series inductance of this cell, L_{te2}, is given by:

$$L_{te2} = L_{sf1} + 2k_{12}\sqrt{L_{sf1}L_{sf2}} + k_{13}\sqrt{L_{sf1}L_{sf3}} . \quad (5)$$

For the end cell of the magnet the total apparent series inductance of this cell, L_{te}, is given by:

$$L_{te} = L_{sf1} + k_{12}\sqrt{L_{sf1}L_{sf2}} + k_{13}\sqrt{L_{sf1}L_{sf3}} . \quad (6)$$

For L_{tc}=62.11 nH, L_{te2}=64.44 nH and L_{te}=99.25 nH, (4)-(6) give $L_{sf1} = 2.196 \bullet L_{tc}$, k_{12}=–0.255 and k_{13}=–0.015. Lleg now represents only series inductance of the legs of the HV and ground plates, and has a value of 50 nH [8].

The original mathematical model of the KAON kicker magnet, in which Ls (Fig. 8) were not mutually coupled, simulated the inductance value of Lleg to be 120 nH: this value was chosen to fit PSpice predictions to measurements. The PSpice prediction for the new mathematical model of the kicker magnet, where Ls is mutually coupled to adjacent cells, is in excellent agreement with measurements [8]. The new model has a significant advantage over the old model, as the derivation of the inductance value is more direct.

C. Deflection Uniformity

The 3D models of the optimized kicker magnet geometry have been used to determine the deflection uniformity. The horizontal deflection angles due to the magnetic and electric fields are summed to determine the total horizontal deflection (section II). The resultant contour plot for a single kicker, normalized to the deflection of protons at the centre of the specified aperture, is shown in Fig. 9. The uniformity is within ±1% over 71.5% of the aperture CSA, in comparison to 83.6% predicted from 2D simulations. The aperture CSA for which the deflection uniformity is within ±2% and ±3% is 85.2% and 89.9%, respectively: these areas are not significantly reduced in comparison with the 2D predictions (section II). Two kickers separated by 20 mm reduce the overall end effects and hence slightly increase the aperture CSA over which a deflection uniformity of ±1%, ±2%, ±3% is achieved to 73.5%, 86.1% and 90.4%, respectively. For Au^{77+} ions the uniformity is ±1%, ±2%, ±3% over 32.9%, 72.5% and 83.3%, respectively, of the aperture CSA.

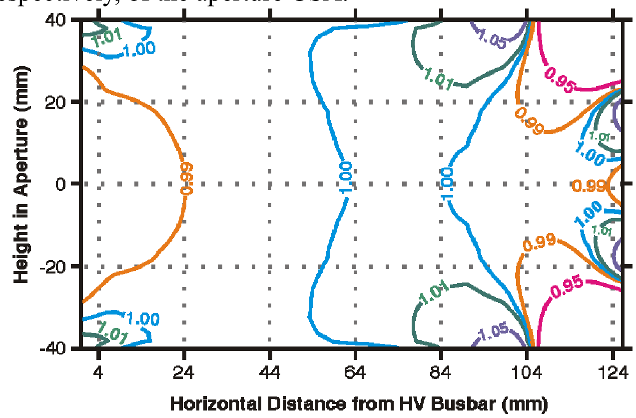

Fig. 9. Normalized contour plot of $\theta_x = \theta_{B,x} + \theta_{E,x}$, for protons, from 3D simulations, for the optimized geometry of a single kicker magnet.

Conclusion

The design goal of ±3% deflection uniformity, for protons, throughout 90% of the aperture CSA has been achieved with the optimized geometry. The ±2% and ±3% deflection uniformities calculated from 2D models is very similar to that determined from 3D models. However the CSA with a ±1% deflection uniformity, calculated from 3D models, is significantly less than that from 2D models.

Acknowledgment

The authors acknowledge the extensive mechanical design work carried out by Tim Emmens.

References

[1] G.D. Wait, M.J. Barnes and H.J. Tran, "Magnetic field in a prototype kicker magnet for the kaon factory", IEEE Trans. on Magnetics, July 1994, Vol. 30, No. 4, pp2118-2121.

[2] M.J. Barnes, G.D. Wait, "Comparison of measured and predicted inductance per cell for a travelling wave kicker magnet", EPAC, Sitges, Spain, 1996, pp2588-2590.

[3] Fiander D., Metzmacher K. and Pearce P., "Kickers and septa at the PS complex, CERN". Kaon PDS Magnet Design Workshop, Oct. 1988, pp71-79.

[4] R.B. Armenta, M.J. Barnes, E.W Blackmore, O. Hadary, G.D. Wait, L. Ahrens, C.J. Gardner, W. Zhang, "Design concept for AGS injection kicker upgrade to 2 GeV", 2005 Particle Accelerator Conference (PAC 2005), May 16-20 2005, Tennessee, USA.

[5] Vector Fields Inc., 1700 North Farnsworth Av., Aurora, IL 60505, USA, www.vectorfields.com

[6] R.B. Armenta, M.J. Barnes, O. Hadary, G.D. Wait, "AGS A10 injection kicker development: deflection angle uniformity and cell inductance based on a two dimensional model of the proposed geometry", TRI-DN-05-01, January 10, 2005.

[7] R.B. Armenta, M.J. Barnes, O. Hadary, G.D. Wait, "AGS A10 injection kicker development: deflection angle uniformity and cell inductance based on a two dimensional model of the optimized geometry", TRI-DN-05-05, February 21, 2005.

[8] M.J. Barnes and G.D. Wait, "PSpice analysis of the AGS A10 kicker magnets", TRIUMF design note TRI-DN-05-15, June 2005.